ELSEVIER

Contents lists available at ScienceDirect

#### Colloids and Surfaces B: Biointerfaces

journal homepage: www.elsevier.com/locate/colsurfb





## Probiotics-embedded polymer films for oral health: Development, characterization, and therapeutic potential

Charlotte Eckermann <sup>a,b</sup>, Christof Johannes Klein <sup>a,b</sup>, Florian Schäfer <sup>c</sup>, Marc Thiel <sup>d</sup>, Agnes-Valencia Weiss <sup>a,b</sup>, Christian Motz <sup>c</sup>, Karen Lienkamp <sup>d</sup>, Matthias Hannig <sup>e</sup>, Marc Schneider <sup>a,b,\*</sup>

- <sup>a</sup> Department of Pharmacy, Biopharmaceutics and Pharmaceutical Technology, Saarland University, Saarbrücken 66123, Germany
- <sup>b</sup> PharmaScienceHub (PSH), Saarbrücken 66123, Germany
- <sup>c</sup> Chair of Materials Science and Methods, Department of Materials and Engineering, Saarland University, Saarbrücken 66123, Germany
- d Chair of Polymer Materials, Department of Materials Science and Engineering, Saarland University, Saarbrücken 66123, Germany
- <sup>e</sup> Clinic of Operative Dentistry, Periodontology and Preventive Dentistry, Saarland University, Homburg 66421, Germany

#### ARTICLE INFO

# Keywords: Oral microbiome Lactobacillus rhamnosus Lactobacillus reuteri Microencapsulation Mucoadhesive polymer films Periodontitis

#### ABSTRACT

The oral microbiome plays a crucial role in maintaining homeostasis, and microbial imbalances contribute to diseases such as periodontitis. Probiotic strains such as Lactobacillus rhamnosus and Lactobacillus reuteri have shown potential in restoring microbial balance in the oral cavity. However, their application remains challenging due to limited survival and adherence under intraoral conditions. Thus, we aimed to develop and evaluate mucoadhesive polymer films for local probiotic delivery. L. rhamnosus and L. reuteri were microencapsulated via spray drying and embedded in films composed of hydroxypropyl methylcellulose-polyvinyl alcohol (HPMC-PVA) and foamed polyvinyl alcohol (PVA). The films were characterized in terms of bacterial viability, tensile strength, folding endurance, and mucoadhesive properties. A proof-of-concept in vivo study was conducted by intraorally exposing enamel samples to two volunteers for eight hours, followed by confocal imaging and morphological analysis of adherent bacteria. Microencapsulation preserved high bacterial viability. The resulting films exhibited suitable mechanical properties and strong mucoadhesion. Biological evaluation revealed clear effects: films containing microencapsulated bacteria led to a statistically significant increase in adherent rod-shaped lactobacilli and a consistent reduction in coccoid bacteria associated with dysbiosis. The foamed PVA formulation showed the most pronounced modulation of the enamel-associated microbiota. These findings demonstrate that probiotic films can enable both bacterial stabilization and effective oral delivery. The system enhances colonization by beneficial bacteria while reducing potentially pathogenic cocci. This approach presents a promising strategy for microbiome-based prevention of oral diseases and merits further clinical investigation.

#### 1. Introduction

The human microbiome, especially the oral microbiome, plays a pivotal role in maintaining oral homeostasis. The dynamic balance between commensal and pathogenic microbes in the oral cavity is essential for oral health [1,2]. Disruption of this equilibrium often leads to diseases including dental caries, periodontitis, and oral candidiasis. Cocci-shaped bacteria are often associated with inflammatory conditions such as periodontitis and contribute to the deterioration of dental

health [3]. This connection has prompted increasing interest in alternative approaches, including probiotic treatments. Strains like *Lactobacillus rhamnosus* and *Lactobacillus reuteri* are known to restore microbial balance. *L. reuteri* has already shown beneficial effects on the oral microbiome in the treatment of periodontitis when incorporated into lozenges [4,5]. Moreover, the successful colonization of the oral cavity by probiotics allowing for interaction between the species is a crucial factor influencing treatment outcomes [6]. *L. reuteri* has been shown to inhibit the growth of oral pathogens (*e.g.*, *S. mutans*, *S. gordonii*,

Abbreviations: AFM, atomic force microscopy; CFU, colony forming units; CLSM, confocal laser scanning microscope; HPMC, Hydroxypropyl methylcellulose; MRS, Man Rogosa Sharpe; NaCl, Sodium chloride; PVA, polyvinyl alcohol; SEM, scanning electron microscope.

<sup>\*</sup> Correspondence to: Biopharmaceutics and Pharmaceutical Technology, Saarland University, Campus C4 1, Saarbrücken D-66123, Germany. E-mail address: Marc.Schneider@uni-saarland.de (M. Schneider).

*P. gingivalis*) and biofilm formation by *S. mutans* [7,8]. Likewise, *L. rhamnosus* exhibits antimicrobial and antiadhesive properties against common oral pathogens such as *S. mutans* and *A. actinomycetemcomitans*, and has been reported to suppress their growth and adhesion to oral surfaces [9]. In addition, *L. rhamnosus* is known to produce bioactive metabolites such as inosine, which have antioxidant, anti-inflammatory, and anti-infective properties that may contribute to microbiome modulation and oral health benefits [10].

Probiotic bacteria were applied for oral health using tablets, capsules, and lozenges, often supplemented with excipients to improve bacterial stability [11,12]. Chewable tablets and lozenges allow direct release of viable bacteria into the oral cavity, thereby enabling local interaction with the microbiota [12]. In addition, probiotic strains have been incorporated into functional foods such as yogurt, kefir, infant formula, nutrition bars, and cereals [6].

To address the challenge of insufficient adhesion in the oral cavity, mucoadhesive polymer films can be used for application. Furthermore, they allow local and thus targeted delivery within the oral cavity. Buccal and sublingual films adhere to the inner cheek and the floor of the mouth, respectively [13], whereas palatal films are designed for the upper oral cavity. This specific local delivery is particularly beneficial in the treatment of oral conditions such as mucositis or periodontitis [14, 15]. The adhesive nature prolongs the residence time at the site of application, preserves local bacterial concentration, enabling sustained release and improving therapeutic efficacy, while reducing dosing frequency and enhancing patient compliance [16].

A wide range of natural and synthetic polymers has been explored for formulating mucoadhesive films. Natural polymers such as chitosan exhibit excellent charge-related mucoadhesive properties [17]. However, its intrinsic antimicrobial activity may limit its suitability for probiotic formulations [18]. Other polysaccharides, including pectin, alginate, and carrageenan, are employed for their gel-forming capacity and biocompatibility, often in combination with synthetic polymers to optimize film characteristics [17,18]. Among synthetic options, commonly used polymers include hydroxypropyl methylcellulose (HPMC), polyvinyl alcohol (PVA), and polyacrylates. HPMC has good film-forming ability, flexibility, and broad compatibility with active agents. It is often combined with PVA to enhance mechanical strength and enable controlled release [19]. Polyacrylates, known for their strong mucoadhesion and hydrogel-forming properties, promote prolonged retention at the application site [19].

Recent advances have demonstrated the feasibility of incorporating living bacteria into mucoadhesive films. For instance, buccal films containing *Lactobacillus brevis* CD2 retained anti-inflammatory activity via arginine deiminase and exhibited strong mucoadhesion [20]. While mucoadhesive films enable site-specific delivery and extended mucosal contact, the disintegration of the probiotic film should not be instant to allow longer retention. To address this, microencapsulation techniques can be employed.

Various biocompatible polymers are described in literature for creating such encapsulation systems. Common materials include alginate and chitosan, known for their gel-forming capacity and mucoadhesive properties [21], as well as gelatin, gum arabic, and maltodextrin, which serve as stabilizers and drying aids [22]. In addition, polymethacrylate-based copolymers such as those of the Eudragit® family are frequently applied as pH-sensitive coatings [23–25]. However, these Eudragits – typically L and S types – have almost exclusively been used in combination with other polymers like chitosan or alginate. Notably, no studies have yet reported the exclusive use of Eudragit® RL or EPO for the microencapsulation of probiotics, and the subsequent local application in the oral cavity.

Although no studies have yet formulated *L. reuteri* or *L. rhamnosus* in mucoadhesive oral films, the suitability of *L. reuteri* for such applications is supported by its well-characterized adhesion properties. A surface protein known as MapA mediates specific and concentration-dependent binding of *L. reuteri* to receptor-like structures on human epithelial cells,

and high-adhesion strains have been shown to bind effectively to both mucus and epithelial surfaces *in vitro* [23].

To the best of our knowledge, no study has combined microencapsulation using Eudragit® S, RL-30D or EPO alone with mucoadhesive film-based delivery for local application in the oral cavity. Previous encapsulation strategies have predominantly relied on polymer combinations and were primarily designed for gastrointestinal release [20,26]. In contrast, the present work introduces a simplified and targeted system specifically adapted to oral conditions, integrating Eudragit®-based microencapsulation with mucoadhesive polymer films. This combination enables both protection and site-specific retention of viable probiotic bacteria. Moreover, the inclusion of a proof-of-concept *in vivo* test under realistic oral conditions adds translational value. Collectively, the study offers a novel formulation approach for local microbiota modulation and presents promising data and starting points for future clinical research.

#### 2. Materials

Freeze-dried *L. reuteri* and *L. rhamnosus* were provided by Lactopia GmbH, Saarbrücken, Germany. MRS broth and MRS agar were purchased from Carl Roth GmbH, Karlsruhe, Germany. Eudragit® EPO, RL30D & S were purchased from Evonik, Essen, Germany. Hydroxypropyl methylcellulose was purchased from Shin-Etsu Chemical, Chiyoda, Japan. Polyvinyl alcohol 18–88 was purchased from Sigma Aldrich, Darmstadt, Germany. Glycerol was purchased from Caelo, Hilden, Germany. Sodium chloride was purchased from Grüssing, Filsum, Germany. Sulfuric acid was purchased from Bernd Kraft, Duisburg, Germany. Branched polyethylenimine was purchased from Sigma Aldrich, Darmstadt, Germany. Mucin from porcine stomach Type II was purchased from Sigma Aldrich, Darmstadt, Germany.

#### 3. Methods

#### 3.1. Microencapsulation

Bacterial microencapsulation was achieved through spray drying, employing polymethacrylate derivatives. Specifically, a 1:1 mixture of Eudragit EPO and Eudragit RL30D, at a total polymer concentration of 10 %, was used. The spray drying process was conducted using a laboratory-scale Mini spray dryer (Buchi B290, Flawil, Switzerland). To reduce thermal stress on the bacteria, a three-way nozzle configuration was used [27]. The polymer solutions, consisting of Eudragit EPO and RL30D dispersed in water, were fed through the outer nozzle, while the purified bacterial suspension was introduced via the inner nozzle. To further mitigate thermal impact, the spray drying process was optimized with an inlet temperature of 55 °C and an outlet temperature of 42 °C, operating at a system pressure of 1.5 bar. The flow rate was maintained at 1 mL/min, with the rotameter set to 60 mm and the aspirator running at full capacity.

#### 3.1.1. Film casting – electromotive film casting device

Polymer films were fabricated using an electromotive film casting system (Coatmaster 510, Erichsen, Hemer, Germany). Aqueous solutions of 1.5 % HPMC and 1.5 % PVA (18–88) were prepared, with glycerol added as a plasticizer at 20 % of the total polymer weight. The solutions were sterilized by autoclaving. (Microencapsulated) bacteria, obtained from liquid cultures, were incorporated into the polymer mixture by gentle stirring. The resulting blend was uniformly spread onto Teflon foils using a squeegee (Erichsen, Hemer, Germany) with a slit width of 1000  $\mu m$ . The films were subsequently dried in a ventilated drying chamber at 37 °C for approximately 1.5 h.

#### 3.1.2. Foamed PVA films

To develop an additional film formulation with a higher loading capacity, foamed PVA films were produced. For this, PVA (18-88) with

20 % (w/w) glycerol, relative to the polymer weight, was cooled to  $4 \,^{\circ}$ C and foamed using a homogenizer (Ultra Turrax, IKA-Werke, Staufen, Germany) for 5 min, with continuous cooling of the sample. The foamed PVA solution was then spread using the electromotive film casting device and dried as previously described. This method resulted in films with a large surface area and increased loading capacity due to a porous structure.

For loading of the foamed films, the pores were filled with microencapsulated bacteria by mechanical mixing. The films were placed in a sample container together with the microencapsulated bacteria and subjected to vortex mixing for 1 min at maximum speed. The loading capacity of the films was determined gravimetrically.

#### 3.2. Film properties

#### 3.2.1. Water content evaluation

The residual water content of the polymer films was determined using a moisture analyzer (Sartorius MA160–1, Sartorius AG, Göttingen, Germany). Films (n =3, from three independent batches per formulation) were heated to 130  $^{\circ}\text{C}$  until a constant weight was reached. The moisture content was recorded automatically by the device.

#### 3.2.2. Mucoadhesion (Mucoadhesive polymer films)

Mucoadhesion was evaluated using two complementary methods, both assessing the interaction between polymer films and mucins derived from porcine stomach tissue at ambient conditions. The first method analyzed interactions over a larger surface area using a tensile test set-up, while the second method focused on smaller surface interactions measured by AFM.

3.2.2.1. Macroscale analysis. For the tensile testing, film samples were cut into  $1~\rm cm^2$  sections and attached to a microscope slide. A counterpart slide coated with mucins was prepared by initially immersing the glass in concentrated sulfuric acid (95–97 %) for cleaning, followed by coating with a polyethyleneimine (PEI) solution in water (2 %). After every step, the slide was washed in MilliQ® water. A mucin suspension (8 % w/w) was then applied, allowing the mucins to adhere to the slide via electrostatic interactions with the PEI. A force-displacement curve was recorded using a tensile test set-up (Instron 8513, Instron GmbH, Darmstadt, Germany). The slides were pressed together with a force of  $5~\rm N$  for  $5~\rm min$  and subsequently separated at a speed of  $0.020~\rm mm/s$  over a distance of  $2~\rm mm$ .

3.2.2.2. Microscale analysis. For probing the intermolecular interactions on a smaller surface area, an atomic force microscope (JPK NanoWizard III, Bruker, Berlin, Germany) was used. The AFM cantilever with the tip having a spherical shape and a diameter of 1  $\mu m$  (Biosphere B1000-FM) was coated with mucins in a manner similar to the microscope slides. The AFM experiment consisted of three phases: in the first phase, the cantilever approached the sample at a speed of 2  $\mu m/s$  with a maximum force of 5 nN. In the second phase, the cantilever remained in contact with the sample for 20 s under the same force, allowing establishment of the interaction. In the final phase, a force-distance curve was recorded by retracting the cantilever from the sample at 2  $\mu m/s$ . The adhesion was then evaluated using the area over the retraction curve to the zero level of the cantilever corresponding to the work of adhesion using JPKSPM Data Processing software.

3.2.2.3. Folding endurance. The strength of pharmaceutical films (such as oral dispersing films) is often characterized for stability by the folding endurance approach [28,29]. The flexibility of the polymer films, both with and without bacterial incorporation, was assessed by measuring folding endurance. The films were repeatedly folded manually at a 180° angle for 300 cycles. Flexibility suitable for oral application was considered sufficient if the films did not rupture during the test.

3.2.2.4. Tensile strength. The tensile strength of the films, both with and without bacterial incorporation, was evaluated using a tensile test set-up (Kappa20, ZwickRoell GmbH & Co. KG, Ulm, Germany) operated in accordance with the DIN EN ISO 527 [30] standards. Film samples were cut to dimensions of  $100\times15$  mm and clamped into the tensile test set-up. The films were subjected to a pulling force at a rate of 50 mm/min until rupture, with no preload applied. The tensile strength was calculated based on the film thickness, which was measured beforehand using an optical microscope. Each formulation was tested five times to ensure reproducibility.

$$Tensile Strength = \frac{Force \ at \ failure}{Cross \ sectional \ area \ of \ film} \times \frac{100}{Film \ thickness} \\ \times \ film \ width \tag{1}$$

#### 3.2.3. Disintegration testing

The dissolution behavior of the films with bacterial loading was assessed. A 1.5 % agarose gel patch was prepared, and the film samples (1  $\mbox{cm}^2$ ) were placed on a polycarbonate membrane with a pore size of 50 nm, followed by incubation on the agarose patch at 36 °C under 100 % relative humidity. Samples were collected at 0, 30, 60 and 120 min. The samples were analyzed using a scanning electron microscope (SEM) (EVO HD15, Carl Zeiss AG, Oberkochen, Germany). For SEM preparation, the samples were mounted on an SEM holder with a carbon adhesive disc, followed by a 100-second gold sputtering process using a Quorum Q150R ES sputter coater (Quorum Technologies Ltd., East Grinstead, UK) to improve conductivity. Images were captured at an acceleration voltage of 5 kV and a magnification of 5000× . Three tests were conducted per formulation.

The pH of the films was measured by dissolving each entire film in a volume of ultrapure water sufficient to achieve a final concentration of 25 mg/mL. The starting water pH was 7.0. After complete dissolution at room temperature, the pH was measured using a Mettler Toledo SevenCompact<sup>TM</sup> pH meter (Mettler-Toledo GmbH, Greifensee, Switzerland) equipped with an InLab® Micro pH electrode (Mettler-Toledo GmbH, Greifensee, Switzerland). Each formulation was tested in triplicate from three independently prepared films (n = 3).

#### 3.3. Cultivation

*L. rhamnosus* and *L. reuteri* were cultured in MRS broth. A single colony from a pregrown MRS-agar plate was selected and inoculated into 30 mL of MRS broth for preculture, followed by overnight incubation at 36 °C under 5 %  $\rm CO_2$ . For the main culture, 1 mL of the preculture was transferred into 250 mL of MRS broth and incubated for 14 h (*L. rhamnosus*) and 16 h (*L. reuteri*) until the stationary phase. The bacterial cells were then harvested by centrifugation at  $5000 \times g$  for 5 min.

#### 3.4. Determination of bacterial activity

The viability of *L. rhamnosus* and *L. reuteri* was determined using the plate count method. Samples containing the bacterial cultures were incubated in a 0.9 % NaCl solution at 37 °C for 45 min to dissolve the polymeric matrix or encapsulating shell. The resulting suspensions were serially diluted in 0.9 % NaCl and subsequently spread on MRS agar plates. After incubation at 36 °C under 5 %  $\rm CO_2$  for 48 h, colony counts were performed in triplicate. The data were expressed in logarithmic form, and the mean values with corresponding standard deviations were calculated.

#### 3.5. Biological testing

The initial testing of the concentration of bacteria per film involved the incorporation of 50, 100 and 150 mg of microencapsulated bacteria (equivalent to 108 mg of dry mass) into each film. The selection of

microencapsulated bacteria was based on their higher loading capacity, which is attributed to the polymers utilized in the encapsulation process. The films were fixed to rehydrated bovine enamel samples and agitated for 2 h in a solution of 2 mL of MilliQ® water at 37 °C, which corresponds to the average volume of saliva present in the oral cavity [31]. This test was conducted in vitro to obviate the need for unnecessary exposure of volunteers. Following the incubation period, the enamel samples were washed with MilliQ® water and stained with Syto 9 (3  $\mu L/mL,\,\lambda=488$  nm excitation,  $\lambda=525$  nm emission) for 15 min. The bacteria were visualized and quantified using confocal laser scanning microscopy (LSM710, AxioObserver, Carl Zeiss AG, Oberkochen, Germany) with an EC Plan-Neofluar 100x/1.3 Oil objective, with 14 CLSM images (8100 μm<sup>2</sup> per image) analyzed per sample. Images were extracted using the Zeiss ZEN blue software with no further processing. Bacterial counts were performed manually. The amount of pure bacteria incorporated into the films was adjusted to match the bacterial content of the corresponding microencapsulated samples.

For biological testing, the film samples were applied to bovine tooth enamel and incubated in the oral cavity of volunteers among the authors for 8 h. The experiments were approved by the ethics committee (Ärztekammer des Saarlandes, Dec. 2024, 196/24). Bovine enamel samples were rehydrated in demineralized water for 24 h, then fixed onto dental splints using a two-component silicone [32]. The films were attached to the enamel, with untreated enamel used as a control on the opposite side of the mouth. Only one type of film sample was tested per subject at a time. The study was conducted with two volunteers. After 8 h of incubation, the samples were rinsed with Milli-Q® water and stained with Syto 9 (3  $\mu$ L/mL,  $\lambda=488$  nm excitation,  $\lambda=525$  nm emission) for 15 min. The samples were subsequently analyzed using CLSM. 14 CLSM images (8100  $\mu$ m² each) were analyzed per sample for quantification of the bacteria.

#### 3.6. Statistical analysis

Statistical analyses were performed using GraphPad Prism (version 10.4.2, GraphPad Software, San Diego, CA, USA). The specific statistical tests applied and the corresponding p-values are provided in the respective figure legends. For comparisons between two groups, unpaired two-tailed t-tests were used. For comparisons involving more than two groups, one-way ANOVA followed by Tukey's multiple comparisons test was applied. All data are presented as mean  $\pm$  standard deviation (SD). Statistical significance was defined as p < 0.05 and indicated as follows: p < 0.05 (\*), p < 0.01 (\*\*\*), p < 0.001 (\*\*\*\*), p < 0.001 (\*\*\*), p < 0.001 (\*\*\*)

#### 4. Results & discussion

#### 4.1. Film casting

In order to facilitate the oral cavity applications, polymer films were fabricated and loaded with bacteria. A variety of methods to produce suitable polymer films were evaluated, including hand casting and the utilization of an electromotive film casting device. The thicker hand-cast films required a drying period of 12 h, whereas the thinner films produced by the film casting device exhibited a shorter drying time of only 1 h at 37 °C. The prolonged drying time of the hand-cast films resulted in a notable loss of activity (data not shown), prompting the decision to proceed with the thinner films produced by the film casting device. Two homogeneous films were produced using an electromotive film casting device. Fig. 1A depicts a transparent polymer film composed of HPMC and PVA, with glycerol (20 % of the total polymer weight) incorporated to ensure adequate flexibility. The thickness of the film was 23.44  $\mu m$ , as determined by using an optical microscope.

Fig. 1B depicts a foamed PVA film. This white polymer film displays pores and a measured thickness of 338  $\mu$ m measured by optical microscopy. For the pores, an average value of  $14.80 \pm 5.25$  per mm² was

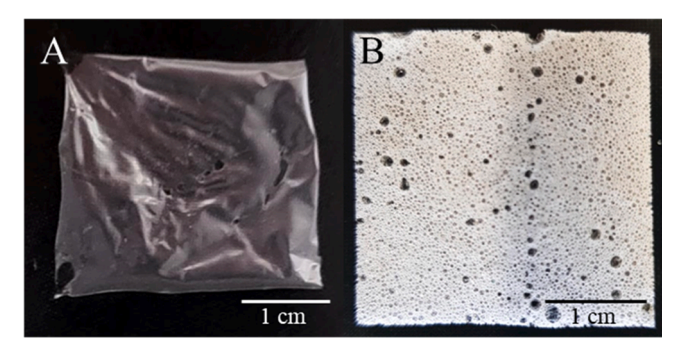


Fig. 1. A Polymer film made of HPMC + PVA using the electromotive film casting device. B Polymer film made from foamed PVA using the electromotive film casting device.

#### determined.

The two distinct types of films produced — transparent HPMC-PVA and foamed PVA — differ significantly in structure and physical properties. The HPMC-PVA film is thin and flexible, as demonstrated by the folding endurance test (see section 4.2.2). Its homogeneity and transparency make it a suitable candidate for mucoadhesive applications in the oral cavity, where a thinner and more flexible film might offer more comfort to the user [33].

The foamed PVA film, which is thicker (338  $\mu m)$  and more porous, shows potential for applications requiring increased bacterial loading. The large pores enable the incorporation of higher quantities of bacteria, which may enhance therapeutic outcomes. However, this is accompanied by a reduction in tensile strength (section 4.2.3), as the pores act as weak points, leading to a lower tear resistance. The flexibility was also sufficient (section 4.2.2). While the HPMC-PVA films exhibited a lower thickness (23.44  $\mu m$ ) compared to Heinemann et al. (~70  $\mu m$ ) [34], Abruzzo et al. (~84  $\mu m$ ) [20] and Lordello et al. (~100  $\mu m$ ) [34], the foamed PVA film reached 338  $\mu m$ . This may affect the film's mechanical performance and disintegration behavior.

#### 4.2. Film properties

#### 4.2.1. Mucoadhesion

The bacteria were embedded into mucoadhesive films designed to extend their residence time at the place of application. A key factor for mucoadhesion is the electrostatic interaction with the negatively charged mucins. Mucoadhesion in the oral cavity was modelled and quantified by measuring the adhesive energy between the films and mucin-coated surfaces both for large and small surface areas. Two different set-ups were used.

Fig. 2A summarizes the adhesion energy data. For the large surface area experiments (1 cm), a tensile test set-up was used. The data indicated that the adhesion energy between the mucin layer and the HPMC-PVA polymer film (1.28  $\times$  10 $^{\text{-4}}$  J) differed only minimally from that between mucin and the foamed PVA film (1.45  $\times$  10 $^{\text{-4}}$  J). As a reference, the interaction between the films and a clean microscope slide was also measured. The interaction between glass and the HPMC-PVA film was  $3.94\times10^{-12}$  J, while the interaction between glass and the foamed PVA film was  $1.76\times10^{-11}$  J.

Interactions on a smaller surface area were measured using atomic force microscopy (AFM) with a mucin-coated tip. As shown in Fig. 2B, the interactions on this scale were significantly weaker. The energy values for the HPMC-PVA film and the foamed PVA film were  $3.63\times10^{-14}\,\rm J$  and  $1.69\times10^{-14}\,\rm J$ , respectively. An uncoated cantilever was used as a reference, but the interactions were so minimal that they could not be quantitatively evaluated. In order to allow a comparison between the different scales, the contact area of the cantilever with the sample was calculated using equation 2. Equation 2 was adapted from the supporting information of Schmitz et al. [35]. It is  $1.33\times10^{-12}\,\rm cm^2$  for the

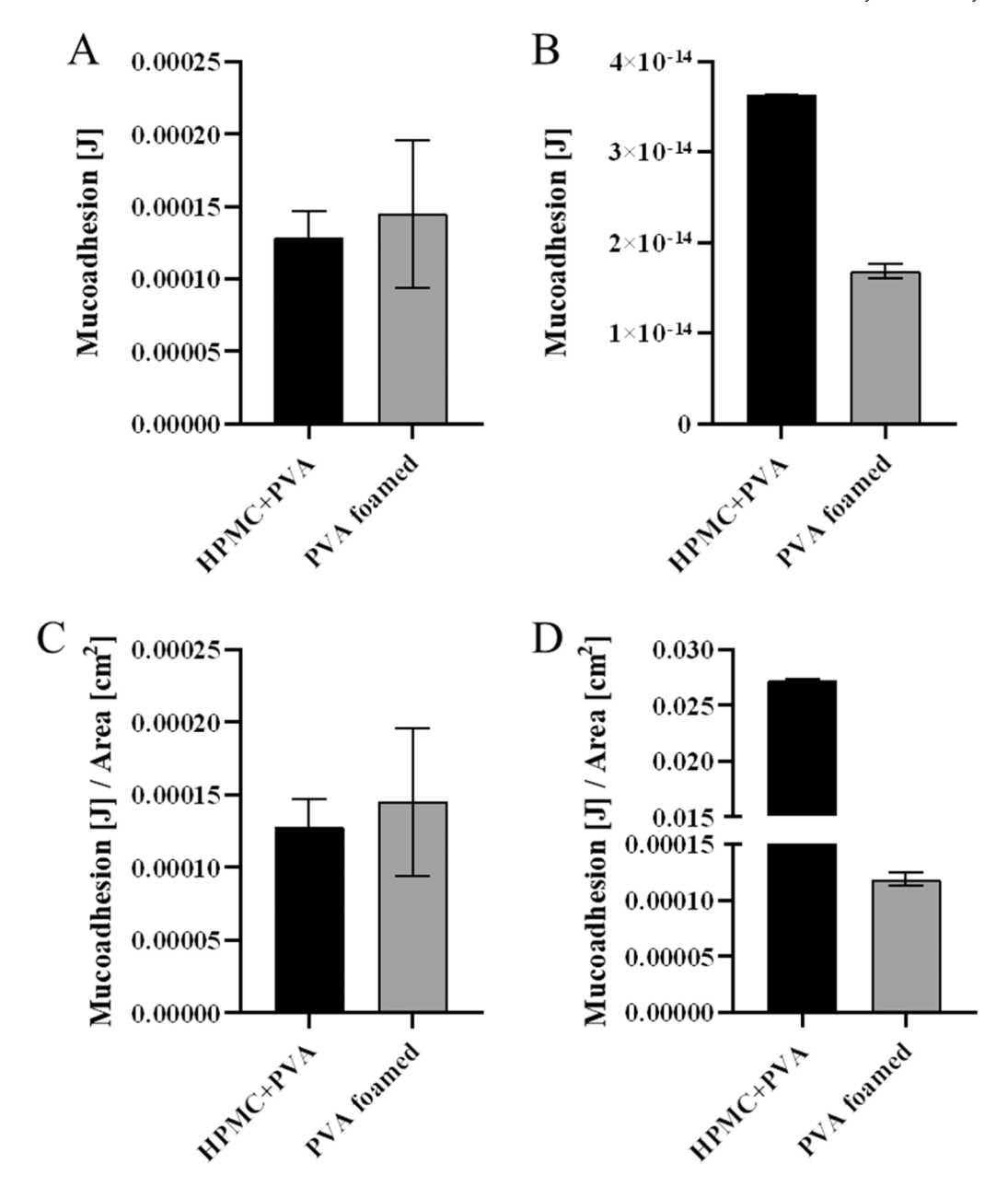


Fig. 2. A: Mucoadhesion was evaluated on a macroscale using a tensile tester. The interaction between the sample and a mucin-coated slide was recorded.  $n=3\pm$  standard deviation. B: Mucoadhesion was evaluated on the microscale using an atomic force microscope (AFM) at ambient conditions. The interaction between the sample and a mucin-coated cantilever was recorded. C: The macroscale testing normalized to the contact area (1 cm²) D: The microscale testing in AFM was normalized by the contact area of the cantilever estimated from the tip indentation,  $n=3\pm$  standard deviation.

HPMC and PVA films and  $1.42 \times 10^{-10}~\text{cm}^2$  for the foamed PVA film. The penetration depth of the cantilever into the polymer film was previously estimated using JPK software enabling extraction from the measured data. The mucoadhesion was adapted to the area (1 cm²) for better comparison (Fig. 2C, D).

$$Area = Radius_{Cantilever}^{2} - (Radius_{Cantilever} - Penetration Depth)^{2}$$
 (2)

Mucoadhesion is a critical factor for ensuring that bacteria remain in the oral cavity long enough to exert their probiotic effects. The results demonstrate that both HPMC-PVA and foamed PVA films exhibit attractive forces higher than the reference reflecting potential mucoadhesion, with energy values (1.28  $\times$  10 $^{-4}$  J and 1.45  $\times$  10 $^{-4}$  J, respectively) indicating strong interactions with the negatively charged mucins. This indicates that either formulation could be employed effectively in oral applications. The values measured are within the ranges provided in literature [36] although the way of providing those

values varies clearly and is not always providing well-normalized data for reasonable comparison. It is noteworthy that the discrepancies between the large and small surface area measurements suggest that the strength of mucoadhesion may exhibit variability depending on the scale of interaction. On a larger scale, there may be a larger number of interactions than on a smaller scale [37–40]. This was demonstrated by the surface normalization, especially for the foamed PVA film but also for the HMPC-PVA films the values were in a similar range. Observed discrepancies may be due to different contact pressures for the different sized samples. This could not be changed due to the different equipment used. The results of both tests demonstrated a notable discrepancy from the reference value in the absence of mucin.

#### 4.2.2. Flexibility

The flexibility of both the HPMC-PVA film and the foamed PVA film was determined via the folding endurance test. As previously

documented in literature, films intended for oral administration must demonstrate the capacity to withstand 300 folds in the same location (Fig. 3) [33].

Both films demonstrated the capacity to withstand 300 cycles of folding without exhibiting any discernible breaks or tears.

#### 4.2.3. Tensile strength

Tear resistance represents a pivotal parameter in the deployment of oral films, as these materials must exhibit adequate tensile strength to withstand use within the oral cavity [33]. The tensile strength of the films was evaluated using a tensile test set-up, in which loaded and unloaded films were analyzed for both strains. The tensile strength was calculated using equation 2.

Fig. 4A presents the tensile strength of the HPMC-PVA films, with and without bacterial loading. The tensile strength of the pure film was 69 Pa, while films loaded with *L. rhamnosus* (50 mg) and *L. reuteri* (50 mg) exhibited tensile strengths of 596 Pa and 522 Pa, respectively. The incorporation of microencapsulated bacteria (100 mg) resulted in a notable alteration in the tensile strength. As illustrated in Fig. 4B, the tensile strength for *L. rhamnosus* decreased to 35 Pa, and for *L. reuteri*, it decreased to 53 Pa. The foamed PVA films, with and without bacterial loading, exhibited the lowest tensile strength. No significant differences in tensile strength were observed based on the bacterial loading. Fig. 4C illustrates that the tensile strength of the pure foamed film was 1.8 Pa, while the tensile strengths of films loaded with microencapsulated *L. rhamnosus* and *L. reuteri* were 1.7 Pa and 1.9 Pa, respectively.

The elevated tensile strength of films containing non-encapsulated bacteria can be ascribed to the intrinsic structural characteristics of the bacteria. The rod-shaped bacterial cells form chains [41], thereby enhancing the stability of the polymer matrix. In contrast, the microencapsulated bacteria, encased in a polymer shell composed of Eudragit EPO and RL 30D, are unable to provide the same degree of organization and thus stabilization of the polymer film. The structure of the microcapsules appears to diminish tensile strength. The foamed PVA films exhibited the lowest tensile strength, which is likely due to the presence of pores, including those at the outer edges, which serve as weak points with a higher likelihood of tearing. The incorporation of microencapsulated bacteria did not result in a notable impact on tensile strength in these foamed systems, as the bacteria were predominantly confined to the pores and did not contribute directly to the polymer matrix.

The data on tensile strength offers crucial insights into the mechanical robustness of the films. The tensile strength of pure HPMC-PVA films was found to be sufficient (69.2 Pa). However, the addition of nonencapsulated bacteria resulted in a clear increase in tensile strength, reaching 596.4 Pa and 521.8 Pa for *L. rhamnosus* and *L. reuteri*, respectively. This is presumably due to the structural characteristics of the bacteria, which form chains within the polymer matrix, thereby reinforcing the film [42–44]. In contrast, films with microencapsulated bacteria demonstrated a reduction in tensile strength, which is likely attributable to the disruption of the ability of the bacteria to form chains due to the encapsulation process, thereby reducing structural integrity.

The foamed PVA films, despite offering advantages in terms of bacterial loading, exhibited the lowest tensile strength (1.8 Pa for the pure

film). The presence of pores weakens the structure, resulting in films that are more prone to tearing. These films may be better suited for applications where large bacterial loadings are needed.

#### 4.2.4. Moisture content of the films

Besides mucoadhesion and the mechanical properties, also the water content of the films is of interest. It might contribute to the mechanical properties. As shown in Fig. 5, the pure polymer film exhibited a moisture content of 10.85 % w/w. Upon incorporation of *L. reuteri* or *L. rhamnosus*, the residual moisture content increased significantly to 17.57 and 13.42 % w/w, respectively. This increase in moisture might be attributed to the hygroscopic nature of the microencapsulated bacterial material and its interaction with the hydrophilic polymer matrix.

Higher moisture content can have both beneficial and detrimental effects on film performance. While a certain level of moisture is necessary for flexibility and probiotic viability, excessive water content may impair mechanical stability or shelf-life. Overall, these values are within the reported ranges for similar films covering lower [20] and higher water amounts [45].

#### 4.2.5. Disintegration of the bacterial films

The scanning electron microscopy (SEM) images illustrated the release of bacteria in all tested formulations. The fastest release occurred from the HPMC-PVA polymer films containing pure L. reuteri (Fig. 6A) and L. rhamnosus (Fig. 6B). At the outset, no free bacteria are discernible. However, after 30 min, the predominant observation is that of free bacteria, with a minimal amount of polymer residues not washed away. This trend persists over time, and by 120 min, only free bacteria are visible.

In contrast, the release of bacteria from the HPMC-PVA films containing microencapsulated *L. reuteri* (Fig. 6C) and *L. rhamnosus* (Fig. 6D) occurred in a more gradual manner. After 30 min, rod-shaped bacteria began to be released, while the microencapsulation structures (red circles) remained visible. With the passage of time, the encapsulation structure diminishes, and by 60 min a greater number of bacteria were released. After 120 min, the encapsulation structures were no longer discernible, and only free rod-shaped bacteria were observed.

The slowest rate of bacterial release was observed in the foamed PVA films. At the designated time point, the film pores were observed to be filled with microencapsulated L. reuteri (Fig. 6E) or L. rhamnosus (Fig. 6F). After 30 min, the microencapsulation structures remained clearly visible (red circles), with only a few free rod-shaped bacteria observed. At this point, the dissolution of the PVA film was evident. After 60 min, dissolution progressed further, releasing more rod-shaped bacteria and reducing the microencapsulation structures. By 120 min, primarily free bacteria and remnants of the encapsulation remain visible.

SEM imaging of the disintegration process provides a visual confirmation of the release dynamics. The HPMC-PVA films exhibited the most rapid release of bacteria, with free L. reuteri and L. rhamnosus observed after 30 min and complete release by 120 min. This indicates a slower release as described for pure HPMC-PVA films only showing times < 10 min [34,46]. This rapid dissolution may be advantageous for applications that require expeditious bacterial delivery. In contrast, the

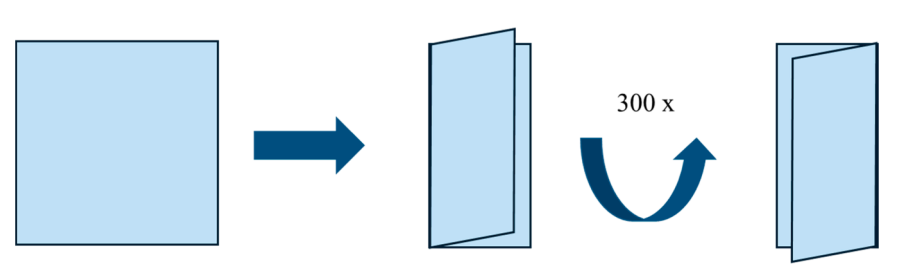


Fig. 3. Schematic illustration of the flexibility test by folding the polymer films by 180° for 300 times.

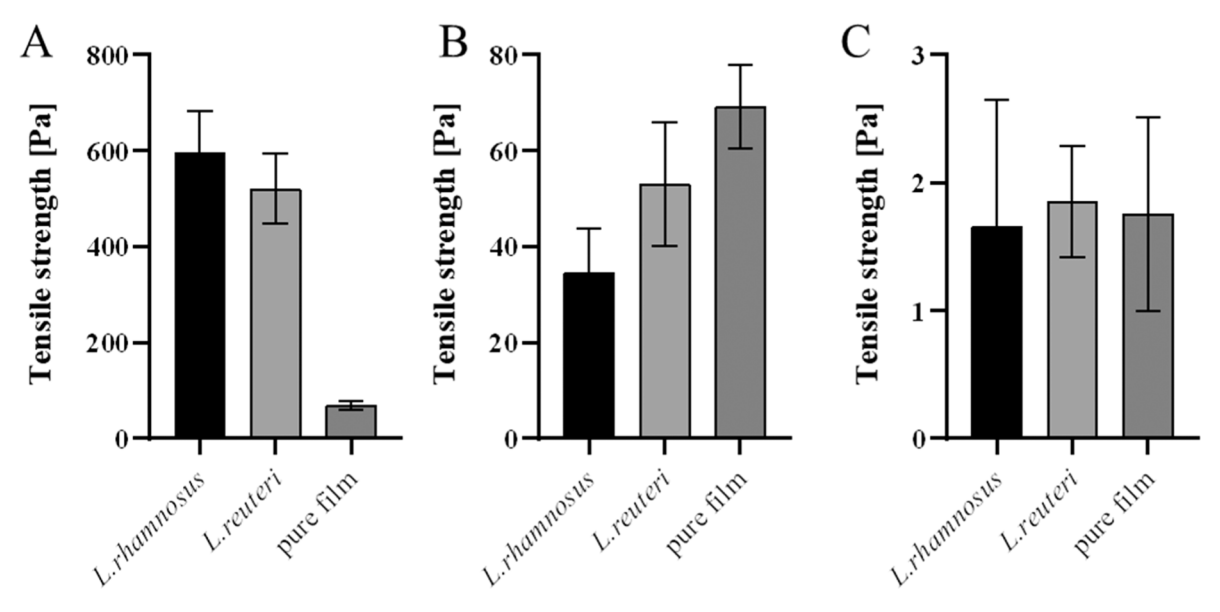
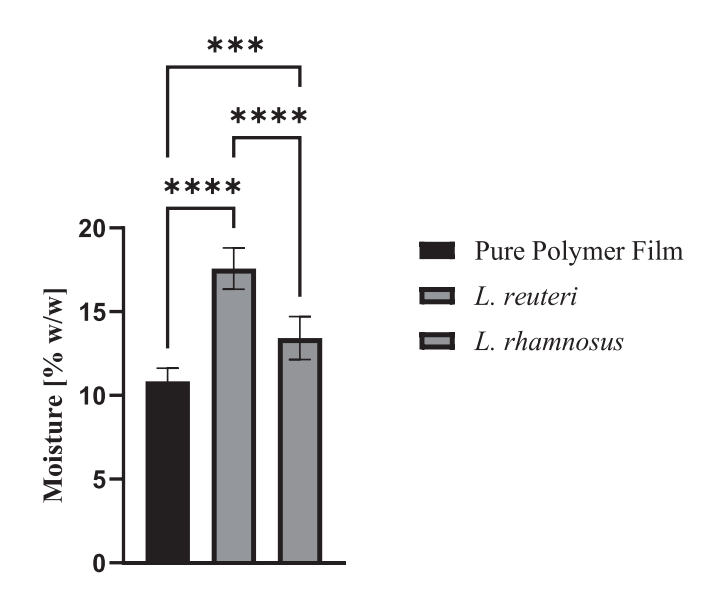


Fig. 4. A: Tensile strength of polymer films made of HPMC and PVA with and without L. rhamnosus and L. reuteri. B: Tensile strength of polymer films made of HPMC and PVA with and without microencapsulated bacteria. C: Tensile strength of polymer films made of foamed PVA with and without microencapsulated bacteria.  $n = 5 \pm \text{standard deviation}$ .



**Fig. 5.** Residual moisture content of polymer films with and without incorporated probiotics. Moisture content [% w/w] was determined gravimetrically using drying at 130 °C. Bars represent mean  $\pm$  SD (n = 3, each performed in triplicate). Statistical analysis was performed using one-way ANOVA followed by Tukey's multiple comparisons test. p < 0.0001 (\*\*\*\*), p < 0.001 (\*\*\*\*).

gradual release from films containing microencapsulated bacteria allows for more precise control of bacterial delivery, which may prolong the therapeutic effect. The slowest release was observed with foamed PVA films, which retained microencapsulated bacteria within their pores even after 60 min. This indicates that foamed PVA films are more suitable for slow-release applications, offering a sustained release of probiotics over time. This is particularly due to the high loading and the higher polymer content of the film. The combination of microencapsulation and film embedding thus also was demonstrated to enable control over the release kinetics. This resembles the extended disintegration times reported by Rebelo et al. (> 20 min) [47] and the prolonged mucosal retention described by Abruzzo et al. [20] due to mucoadhesive contact as a means of sustained delivery.

4.2.5.1. pH determination. Besides the disintegration behavior of the polymeric films, we also tested the resulting pH of the solution. The pH measurement of fully dried films rehydrated in ultrapure water (25 mg/mL) revealed clear differences depending on the encapsulated bacterial strain. The pure polymer film (no bacteria added) exhibited a nearly neutral pH of  $\sim$ 6.9. In contrast, films containing *L. reuteri* and *L. rhamnosus* showed significantly lower pH around 5.6, indicating a pronounced acidification (Fig. 7).

The differences between the placebo film and both probiotic formulations were highly significant (p < 0.0001), while no significant difference was observed between the different bacteria, suggesting comparable acidifying effects from both strains. This acidification may result from metabolic activity during film processing, the release of acidic cellular components, or a strain-dependent shift in the buffering capacity of the film.

The observed drop in pH could enhance the antimicrobial potential of the films, particularly against pH-sensitive oral pathogens, and may complement the probiotic action by creating an environment unfavorable to harmful bacterial colonization.

Taken together, these findings demonstrate that incorporating probiotic bacteria into the polymer matrix significantly alters the chemical characteristics of the system – most notably the pH – which may contribute to the overall biofunctional efficacy of the delivery film.

#### 4.3. Biological analysis

#### 4.3.1. Bacterial activity

For the bacteria in the final formulation to be effective when used in the oral cavity, it is essential that they exhibit sufficient activity.

The activity of *L. rhamnosus* and *L. reuteri* was quantified by determining the number of colony-forming units (CFU) per g. Activity measurements were performed immediately with samples after cultivation to the stationary phase, after microencapsulation by spray drying, and samples taken from the polymer film, via the plate count method.

*L. reuteri* exhibited a statistically significant reduction in viability of  $\sim 0.22$  log units after spray drying (p < 0.05) compared to freshly cultivated cells (Fig. 8). Similarly, *L. rhamnosus* showed a decrease of approximately 0.30 log units (p < 0.05). These modest losses indicate that spray drying, although not entirely benign, is relatively mild in its effect on bacterial survival. The use of a three-way nozzle and the rapid

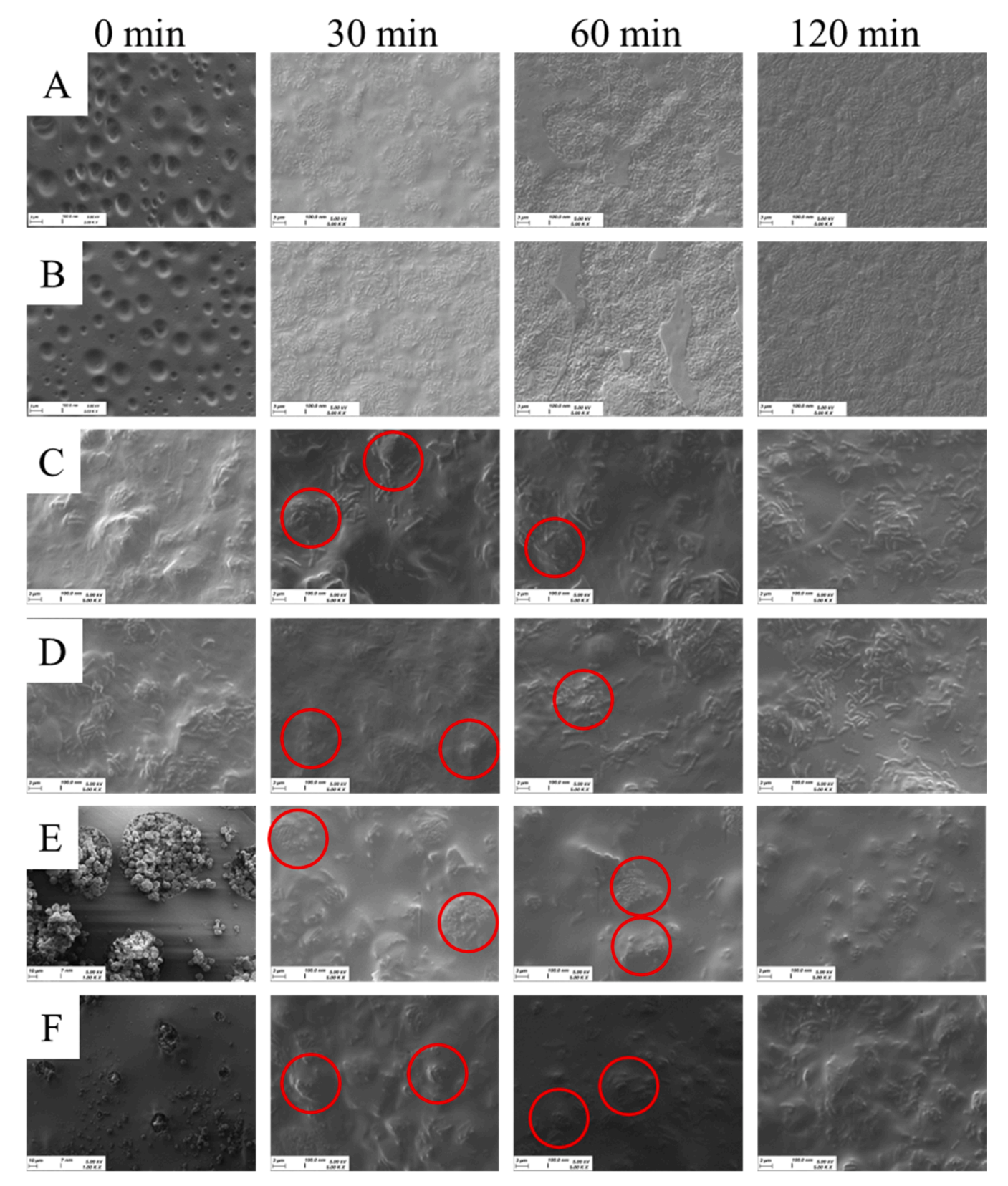
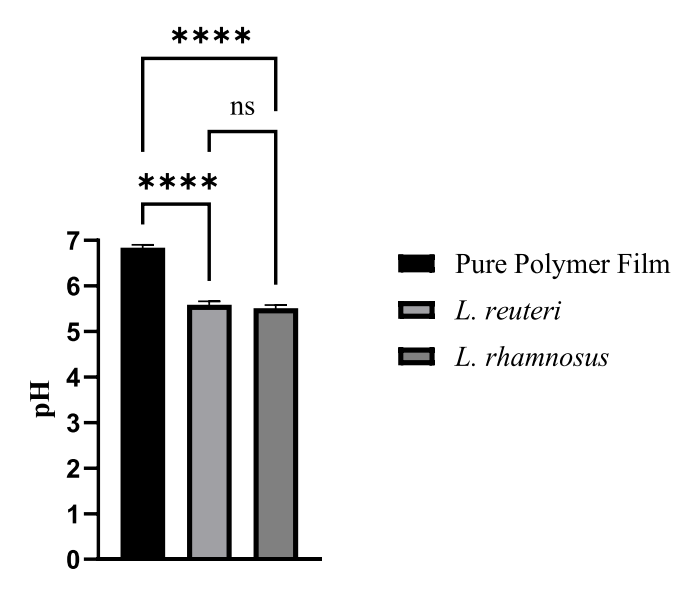


Fig. 6. Series of SEM micrographs illustrating the dissolution of polymer films on 1.5 % agarose gel patches at 36 °C and 100 % relative humidity. Samples were imaged after different incubation times at 0 min, 30 min, 60 min and 120 min. A: HPMC-PVA film + L. reuteri, B: HPMC-PVA film + L. rhamnosus, C: HPMC-PVA film + microencapsulated L. reuteri, F: foamed PVA film + microencapsulated L. reuteri, F: foamed PVA film + microencapsulated L. rhamnosus. The remaining microencapsulated structure is indicated by red circles.



**Fig. 7.** pH values of rehydrated polymer films (25 mg/mL in ultrapure water, pH 7.0) containing either no bacteria (pure polymer film), *L. reuteri*, or *L. rhamnosus*. Data represent mean  $\pm$  SD (n = 3; each from three independent batches). Statistical analysis was performed using one-way ANOVA with Tukey's multiple comparisons test. p < 0.0001 (\*\*\*\*); ns = not significant.

drying process appear to keep thermal damage low, contributing to the overall preservation of viability in both strains.

Direct incorporation into polymer films without prior encapsulation, both *L. reuteri* and *L. rhamnosus* showed a moderate but significant loss of viability similar to work with different bacteria in literature [20,34,46]. For *L. reuteri*, the decrease was  $\sim$ 0.33 log units (p < 0.01), while *L. rhamnosus* showed a decline of  $\sim$ 0.42 log units (p < 0.01). These results suggest that the film-forming process poses a larger stress on the cells than spray drying. This might be due to the longer drying time.

When combining both processes – microencapsulation followed by incorporation into a polymer film – a highly significant reduction in viability was observed for both strains (*L. reuteri*:  $\sim$ 6.0 log units (p < 0.0001), *L. rhamnosus*: 1.15 log units (p < 0.0001)). These results suggest that the combination of spray drying and film integration

imposes cumulative stress. L. reuteri appears more sensitive to this combined burden than L. rhamnosus.

When comparing microencapsulated bacteria to those embedded directly into films without encapsulation, no statistically significant differences in viability were observed for either strain (p>0.05) (*L. reuteri* dropped by  $\sim 0.11$  log units, and *L. rhamnosus* dropped by  $\sim 0.12$  log units). These findings indicate that each strategy imposes a comparable stress level on the bacteria. This suggests that either encapsulation or direct embedding may be used independently without major differences in survival outcome – though other factors like targeted release or mucoadhesion might still influence the overall effectiveness of each approach.

When comparing microencapsulated bacteria before and after film incorporation, a strong viability loss was observed. For *L. reuteri*, viability dropped by  $\sim\!5.8$  log units (p<0.0001), indicating that film formation caused additional stress, which encapsulation could not mitigate. For *L. rhamnosus*, the reduction was less pronounced ( $\sim\!0.85$  log units) but still statistically significant (p<0.01). These findings confirm that the protective effect of microencapsulation is not sufficient to preserve bacterial viability under subsequent film-forming conditions.

Also comparing the effect of *L. reuteri* and *L. rhamnosus* to the pure film formation process without microencapsulation showed similar effects. *L. reuteri's* activity declined by  $\sim$ 5.7 log units (p < 0.0001), and *L. rhamnosus'* activity declined by  $\sim$ 0.73 log units (p < 0.01). These results indicate that the process of encapsulation followed by film formation does not confer an additive protective effect – in fact, for *L. reuteri*, it may exacerbate viability loss.

In comparison, the polymer films developed in this study showed viability reductions for L. reuteri ( $\sim$ 0.33 log units) and for L. rhamnosus ( $\sim$ 0.42 log units), exceeding those reported by Heinemann and Abruzzo [20,46] but remaining substantially lower than the 84.5 % loss observed by Lordello et al. [34]. For the combined processes of film formation and spray drying no literature data was available.

#### 4.3.2. Influence of bacterial concentration

Various concentrations of microencapsulated bacteria were incorporated into polymer films to determine the optimal bacterial loading. The goal was to produce a stable film with the highest possible bacterial content.

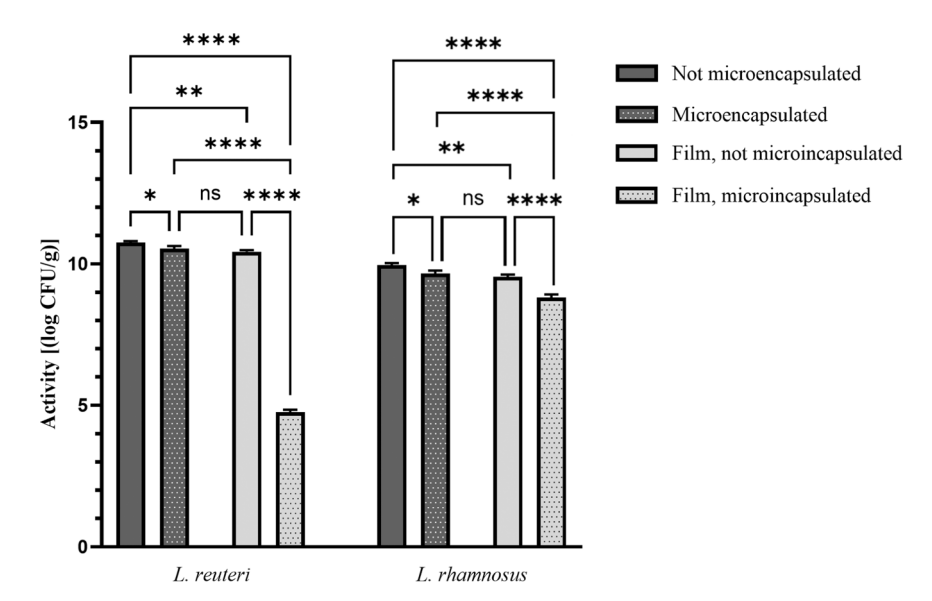


Fig. 8. Survival of Lactobacillus reuteri and Lactobacillus rhamnosus under different processing conditions. Bacterial activity was measured as log(CFU/g) after four treatments: (1) not microencapsulated, (2) microencapsulated, (3) incorporated into a polymer film without prior encapsulation, and (4) incorporated into a polymer film after microencapsulation. Data are presented as mean  $\pm$  standard deviation (n = 3). Statistical analysis was performed using separate one-way ANOVA tests for each bacterial species, followed by Tukey's multiple comparisons test. p < 0.05 (\*), p < 0.01 (\*\*\*), p < 0.0001 (\*\*\*\*); ns = not significant.

For both *L. rhamnosus* and *L. reuteri*, an increase in the quantity of microencapsulated bacteria from 50 mg to 100 mg and 150 mg per film resulted in a corresponding rise in the number of bacteria adhering per enamel piece (Fig. 9). Although the differences were not statistically significant due to high standard deviations, a trend toward increased bacterial adhesion with higher concentrations was observed. The film containing 150 mg of bacteria exhibited the highest bacterial adhesion; however, its structural stability was insufficient.

During the manufacturing process, the film could not be harvested in a single piece from the Teflon foil, rendering it unsuitable for further tear resistance testing. Consequently, subsequent experiments were conducted using films containing 100 mg of microencapsulated bacteria, which provided an appropriate balance between bacterial incorporation and film stability. These films were also employed for the subsequent tests. The mass of bacteria in the polymer films containing pure cultures was adjusted to achieve the desired result, with 50 mg (dry mass) of bacteria per polymer film (108 mg dry mass) utilized.

The film instability found supports the finding from the tensile testing that the film strength decreases with loading of microencapsulated bacteria. It also reveals that increasing the amount of probiotics can significantly impair the structural stability of the carrier films. Similar behavior is described in literature for pullulan/starch polymer films [48]. Therefore, a functional compromise between sufficient probiotic dose and structural resilience of the matrix seems necessary.

#### 4.3.3. Incubation in oral cavity

In all subsequent experiments, untreated controls consistently exhibited colonization by coccoid bacteria. Such morphologies are typical of oral colonizers and have been associated with species like *Streptococcus mutans*, *S. oralis*, and *S. sobrinus*, known for their cariogenic and opportunistic pathogenic potential [49–51].

4.3.3.1. Pure polymer film. To assess the effect of the polymer film on bacterial adhesion under real conditions, the pure polymer film composed of HPMC and PVA was incubated in the oral cavity of two volunteers for 8 h. The bacteria were imaged using CLSM.

All observed bacteria exhibited coccoid morphology, consistent with early supragingival colonizers in the absence of probiotic intervention [49–51]. Visual inspection of CLSM images revealed a reduced bacterial coverage on enamel specimens treated with the unloaded polymer film compared to untreated reference samples, most notably in volunteer 2 (Fig. 10). Quantitative analysis substantiated the visual impression. For volunteer 2, the reduced bacterial adhesion was significant (p < 0.01).

Also, for volunteer 1 a clear trend towards reduced adhesion was observed although not statistically significant (p = 0.2895) (Fig. 10E).

These results indicate that the HPMC–PVA film alone, even without bacterial loading, can reduce bacterial colonization on enamel surfaces under intraoral conditions. Taken together, these findings show that the unloaded polymer film has a mild, potentially protective effect.

4.3.3.2. Polymer film containing microencapsulated bacteria. The polymer film containing microencapsulated bacteria was incubated in the oral cavity of two volunteers for 8 h, following the same procedure as for the pure polymer film. The samples were analyzed by CLSM, as previously described.

Representative CLSM images of enamel samples treated with polymer films containing microencapsulated *L. reuteri* (Fig. 11, Panels B and D) or *L. rhamnosus* (Fig. 11, Panels F and H) show the presence of rodshaped bacteria, which were not detectable in untreated controls (Fig. 11, Panels A, C, E, G). All untreated samples predominantly exhibited coccoid morphologies, suggesting a native oral biofilm dominated by spherical bacteria as previously described in literature [52].

In contrast, samples treated with probiotic-loaded films displayed a marked increase in rod-shaped bacteria, coinciding with a substantial reduction in coccoid cells. This shift in morphology is consistent across both strains and both volunteers, indicating successful release and adhesion of the encapsulated lactobacilli.

Quantitative analysis (Fig. 11, Panels I and J) supports these observations. For both *L. reuteri* and *L. rhamnosus*, the number of adherent cocci was significantly reduced in the treated groups compared to the untreated controls (p < 0.0001 to p < 0.01). Simultaneously, a significant increase in rod-shaped bacteria was observed in all treated samples (p < 0.001 to p < 0.0001), verifying that the microencapsulated lactobacilli adhered effectively to the enamel surfaces.

Compared to the pure polymer film without probiotics (Fig. 10), which showed only a moderate reduction in adherent bacteria, the probiotic-loaded films in Fig. 11 induced a statistically significant shift in microbial composition. This highlights that the observed reduction in coccoid bacteria and increase in rod-shaped lactobacilli is not attributable to the film material alone, but rather to the delivery of probiotics.

4.3.3.3. Polymer film containing pure bacteria. In addition to testing the polymer film with microencapsulated bacteria, a polymer film containing non-encapsulated bacteria was also applied to tooth enamel and evaluated. As with the preceding films, the film was incubated for eight

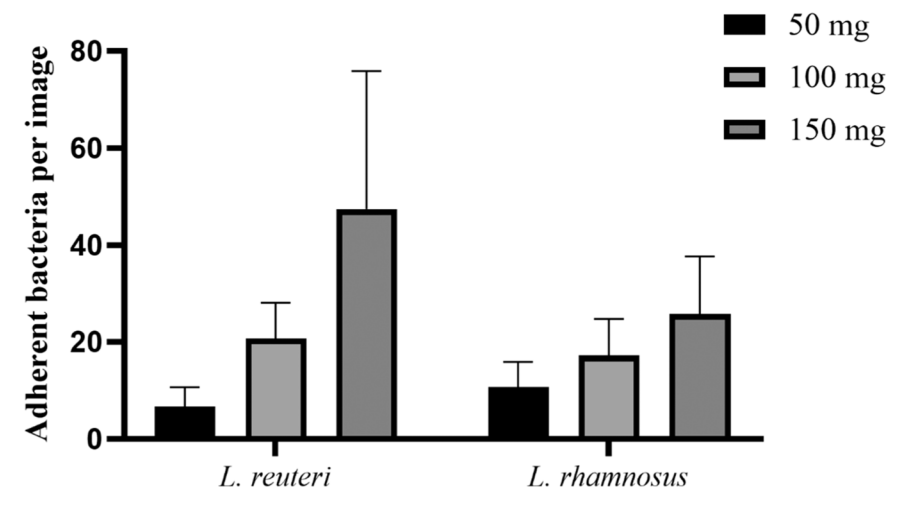


Fig. 9. Adherence of *L. reuteri* and *L. rhamnosus* to bovine enamel after application of polymer films containing 50, 100, or 150 mg of microencapsulated bacteria. Data represent the number of adherent bacteria per CLSM image (8100  $\mu$ m<sup>2</sup>), shown as mean  $\pm$  SD (n = 3). Statistical analysis was performed using separate one-way ANOVA tests for each bacterial species, followed by Tukey's multiple comparisons test.

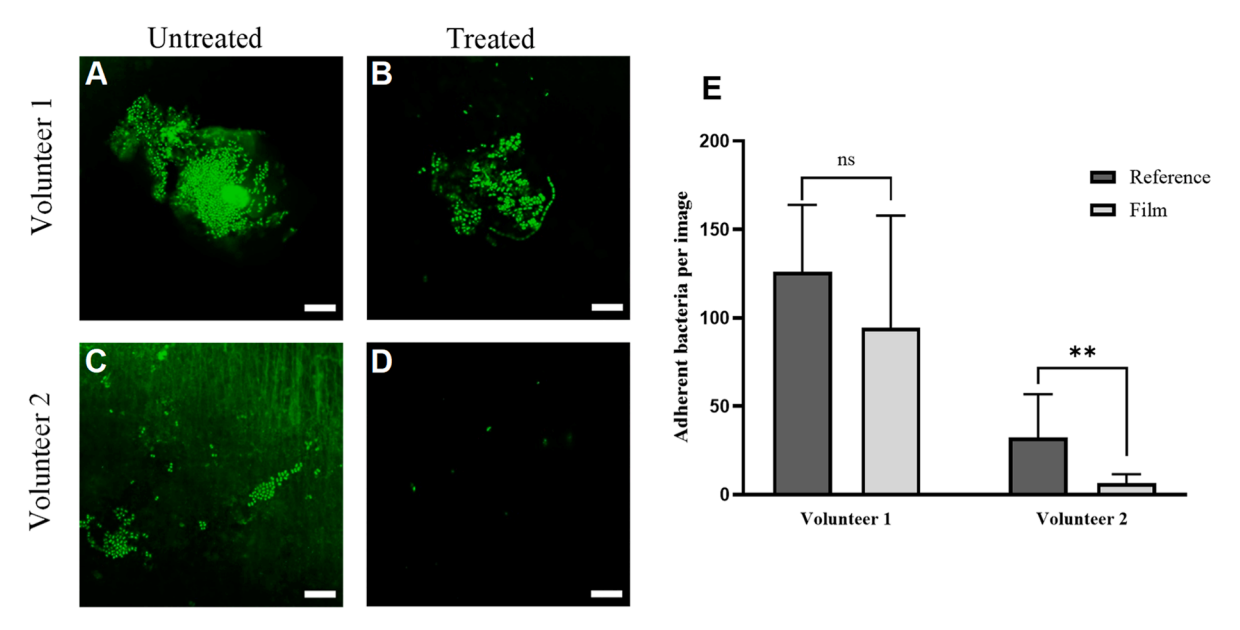


Fig. 10. Adherence of oral bacteria to enamel after *in vivo* application of unloaded HPMC-PVA films. CLSM images of enamel samples from two volunteers after 8 h of intraoral exposure, comparing untreated (A, C) and polymer film-treated specimens (B, D). Scale bars represent 10  $\mu$ m. Panel E shows the quantification of adherent bacteria per CLSM image (8100  $\mu$ m²), presented as mean  $\pm$  SD (n = 3). Statistical analysis was performed using unpaired two tailed t tests. p < 0.01 (\*\*); ns = not significant.

hours in the oral cavities of two volunteers, and bacterial visualization was performed using CLSM.

Representative CLSM images show that application of polymer films containing non-encapsulated *L. reuteri* (Fig. 12, Panels B and D) or *L. rhamnosus* (Fig. 12, Panels F and H) resulted in the presence of rod-shaped bacteria (highlighted with red circles) on the enamel surfaces, which were absent in the corresponding untreated control samples (Fig. 12, Panels A, C, E, G). The untreated enamel samples primarily exhibited coccoid morphologies.

Quantitative analysis (Fig. 12, Panels I and J) confirmed a significant reduction in coccoid bacteria for *L. reuteri* treatment in volunteer 1 (p < 0.01), while no significant difference was observed in volunteer 2. For both volunteers, the number of rod-shaped bacteria increased significantly upon treatment (p < 0.01 for volunteer 1, p < 0.05 for volunteer 2). Similar results were observed for *L. rhamnosus*: coccoid adhesion was significantly reduced only in volunteer 1 (p < 0.0001), while the reduction in volunteer 2 did not reach significance. However, in both volunteers, adhesion of rod-shaped bacteria was significantly enhanced (p < 0.001).

When compared to the results from films containing microencapsulated bacteria (Fig. 11), the probiotic effects of the non-encapsulated formulations were less pronounced. While both systems facilitated the adhesion of rod-shaped lactobacilli and partially reduced native coccoid bacteria, the extent of these effects was greater and more consistent for microencapsulated bacteria. In particular, the coccoid suppression was more reliable with encapsulated strains, and the relative abundance of rods was markedly higher. This difference indicates a functional advantage of microencapsulation in delivering probiotics to the enamel surface.

In summary, these findings show that although probiotic activity is retained without encapsulation, the consistency and strength of the effect are reduced compared to the microencapsulated formulation.

4.3.3.4. Increased loading of microencapsulated bacteria. One strategy to increase bacterial loading involved utilizing a foamed PVA film (Fig. 1B), where the film's pores were loaded with bacteria. The pores were then sealed with a polymer film composed of PVA and HPMC. This was achieved by partly dissolving the film in water and subsequently fixing it to the underlying foamed film.

The presented CLSM images show that application of foamed PVA films containing microencapsulated *L. reuteri* (Fig. 13, Panels B and D) or *L. rhamnosus* (Fig. 13, Panels F and H) resulted in the presence of rod-shaped bacteria on enamel surfaces, which were absent in the corresponding untreated control samples (Fig. 13, Panels A, C, E, G). The untreated enamel specimens primarily exhibited coccoid morphologies, representative of the native oral microflora.

Quantitative analysis (Fig. 13, Panels I and J) confirmed a significant reduction in the number of coccoid bacteria for both strains and both volunteers (p < 0.01 for volunteer 1, p < 0.0001 for volunteer 2). Likewise, for both strains and both volunteers, adhesion of rod-shaped bacteria increased significantly upon treatment (p < 0.0001 for volunteer 1, p < 0.001 for volunteer 2), indicating efficient release and adherence of the encapsulated lactobacilli.

When compared to the results from non-foamed polymer films (Fig. 11 and 12), the probiotic effects of the foamed PVA formulation were more pronounced. The number of adherent rods was higher, and coccoid suppression was more consistent and substantial. This suggests that the porous architecture enabling increased bacterial loading led to superior colonization.

4.3.3.5. Comparative analysis of the tested polymer film formulations for in vivo probiotic delivery. To systematically assess the performance of different polymer film systems for oral probiotic delivery, four distinct formulations were evaluated under *in vivo* conditions: an unloaded polymer film (Fig. 10), a film containing non-encapsulated bacteria (Fig. 12), a film with microencapsulated bacteria in a non-foamed matrix (Fig. 11), and a microencapsulated probiotic film embedded in a foamed PVA scaffold (Fig. 13). Each formulation was tested in an 8-hour intraoral exposure model in two volunteers, followed by CLSM-based visualization and quantification of adherent bacteria classified by morphology.

The unloaded HPMC-PVA film (Fig. 10) served as a baseline control to isolate the effect of the polymer matrix alone. While this formulation showed a reduction in coccoid bacteria in one volunteer (p < 0.01), the effect was not consistent across individuals. This suggests a limited, volunteer-dependent antiadhesive potential of the film matrix, likely due to surface modification.

In contrast, microencapsulated bacteria delivered in a polymer film

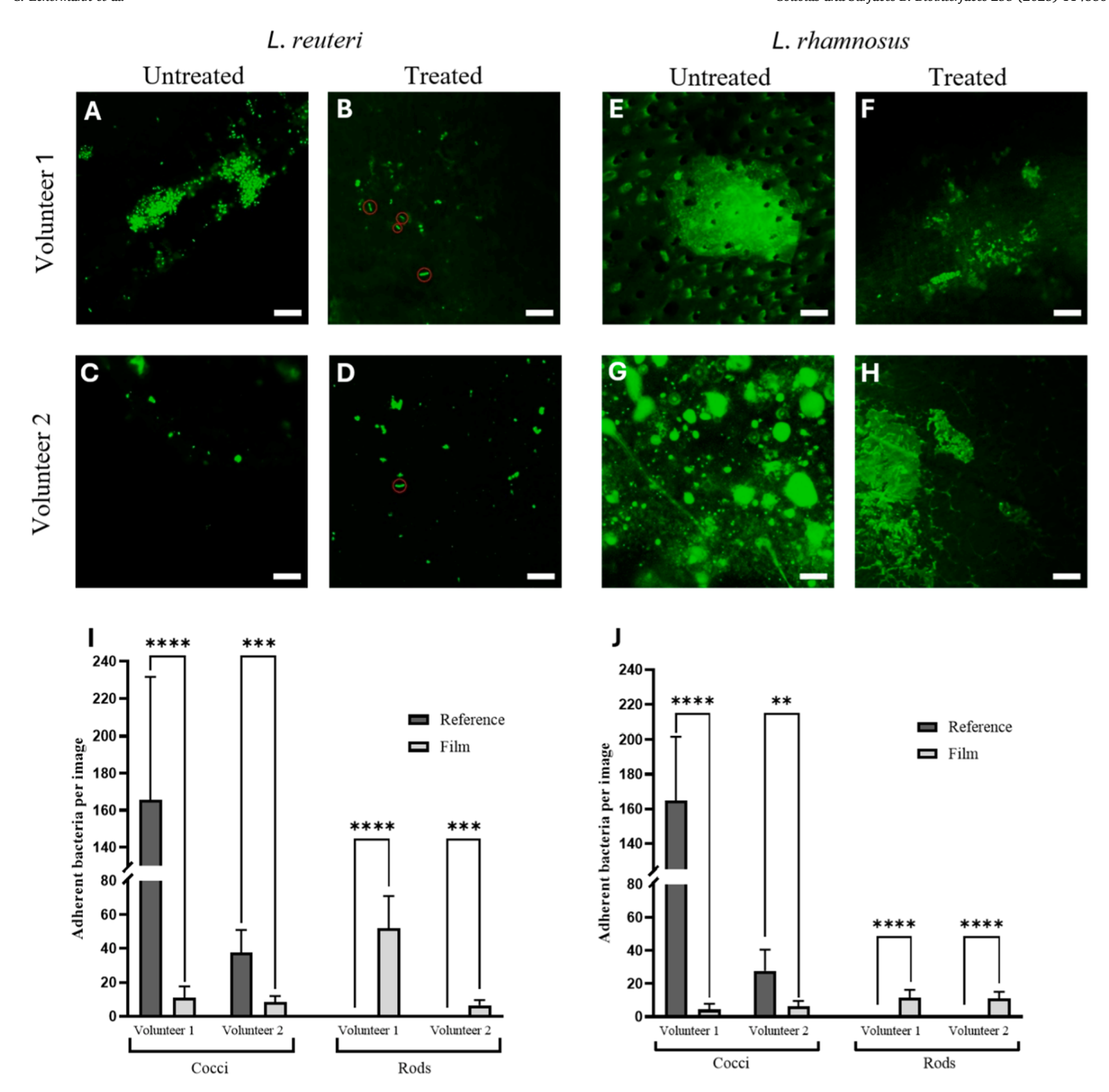


Fig. 11. Bacterial adherence to enamel after HPMC-PVA film application containing microencapsulated *L. reuteri* or *L. rhamnosus*. Representative CLSM images show enamel samples from two volunteers after 8 h of intraoral exposure. Panels A–D display samples treated with films containing *L. reuteri* (A, B: untreated; C, D: treated), while panels E–H show samples for *L. rhamnosus* (E, F: untreated; G, H: treated). Exemplified rod-shaped bacteria are highlighted in circles in Panels B, D, F and H. Panels I and J show the quantification of adherent coccoid and rod-shaped bacteria per image (8100 μm²) for enamel specimens treated with polymer films containing *L. reuteri* (Panel I) and *L. rhamnosus* (Panel J), respectively. Data are presented as mean  $\pm$  SD (n = 3). Statistical analysis was performed using unpaired two-tailed t tests. p < 0.01 (\*\*\*), p < 0.001 (\*\*\*\*), p < 0.0001 (\*\*\*\*); ns = not significant. Scale bars represent 10 μm.

(Fig. 11) exhibited improved performance. In both volunteers and for both tested strains (L. reuteri and L. rhamnosus), a statistically significant increase in rod-shaped bacteria was accompanied by a consistent reduction in coccoid morphologies. These results validated the protective and stabilizing effect of microencapsulation.

Furthermore, the film containing non-encapsulated *Lactobacillus* strains (Fig. 12) also demonstrated clear evidence of probiotic adhesion. Rod-shaped bacteria were detected exclusively in the treated samples, and partial displacement of native coccoid bacteria was observed. However, the overall effects were inconsistent: coccoid suppression

reached statistical significance only in one of two volunteers per strain, and rod-shaped adhesion was generally lower than with encapsulated formulations. These findings point to a limited efficiency of non-encapsulated bacteria. However, the low number of volunteers might mask this.

The highest efficacy was achieved with the foamed PVA film containing microencapsulated bacteria (Fig. 13). This formulation resulted in the largest number of adherent rod-shaped bacteria and the most consistent and substantial reduction in coccoid cell counts across both strains and both volunteers. The porous architecture allowed to deliver a

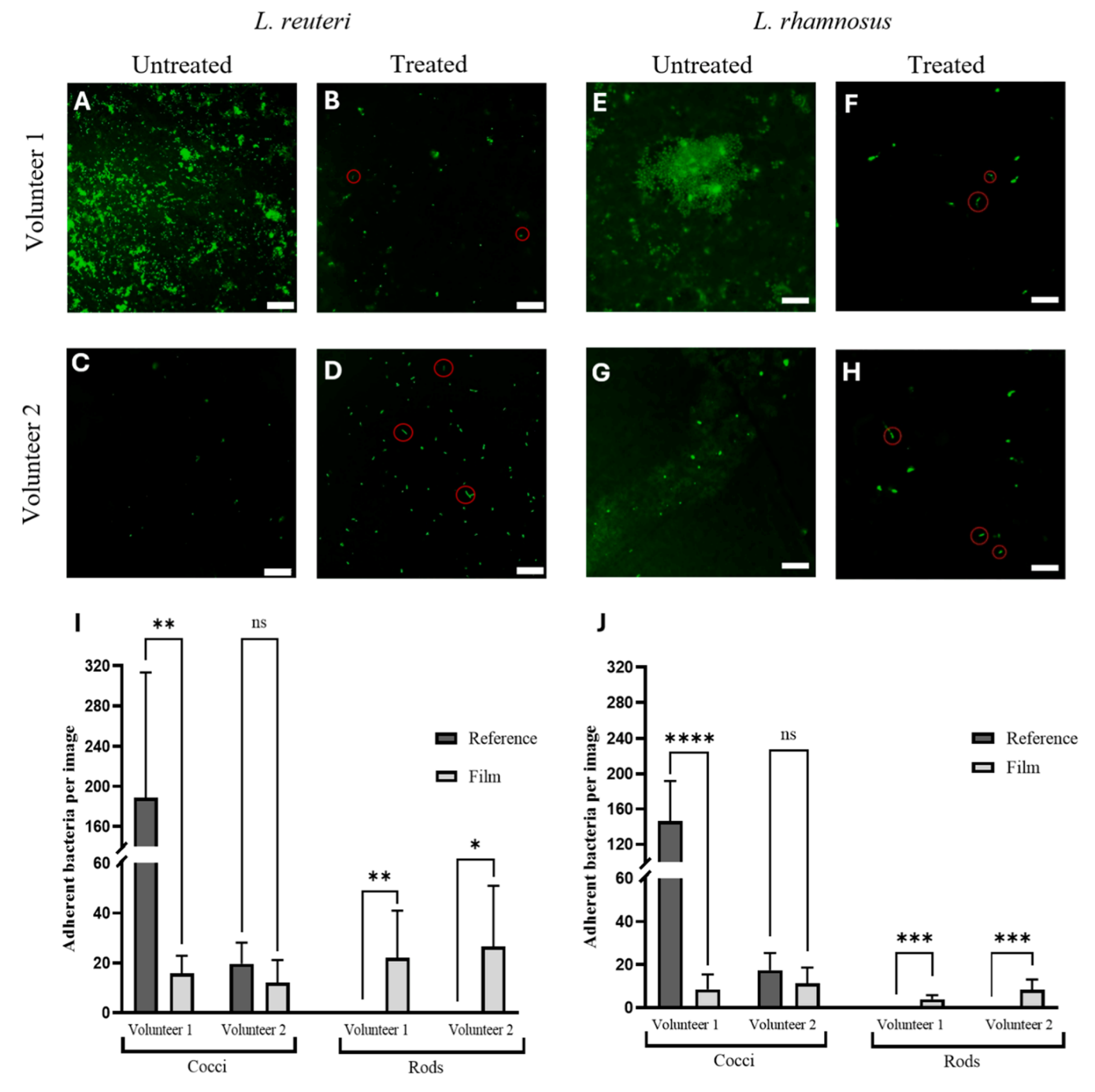


**Fig. 12.** Bacterial adherence to enamel following application of HPMC-PVA films containing non-encapsulated *L. reuteri* or *L. rhamnosus*. Representative CLSM images show enamel samples from two volunteers after 8 h of intraoral exposure. Panels A–D display samples treated with films containing *L. reuteri* (A, B: untreated; C, D: treated), while Panels E–H show samples for *L. rhamnosus* (E, F: untreated; G, H: treated). Circles are highlighting examples for rod-shaped bacteria after treatment. Panels I and J show the quantification of adherent coccoid and rod-shaped bacteria per image (8100 μm²) for enamel specimens treated with films containing *L. reuteri* (Panel I) and *L. rhamnosus* (Panel J), respectively. Data are presented as mean  $\pm$  SD (n = 3). Statistical analysis was performed using unpaired two-tailed t tests. p < 0.05 (\*), p < 0.01 (\*\*\*), p < 0.001 (\*\*\*\*), p < 0.0001 (\*\*\*\*); ns = not significant. Scale bars represent 20 μm in panels A–D and 10 μm in Panels E–H.

higher number of bacteria aligning with a stronger effect. Importantly, the combination of encapsulation and structural optimization provided synergistic benefits in terms of colonization efficiency and displacement of endogenous biofilm constituents.

In summary, the data clearly demonstrate that both microencapsulation and film architecture are critical determinants of successful probiotic delivery in the oral cavity. Unloaded films may offer limited passive antiadhesive effects, but active microbiome modulation requires probiotic delivery. Encapsulation significantly enhances adherence and

stability, while the addition of a foamed matrix maximizes delivery efficiency. These insights are essential for the rational design of next-generation oral probiotic systems with clinical potential.

These findings are consistent with previous reports demonstrating the probiotic potential of *Lactobacillus reuteri*. Liu et al. [53] describe that *L. reuteri* can continuously increase the number of beneficial bacteria in the oral cavity, thereby contributing to the restoration of a balanced microbiome [53]. Moreover, regular intake of *L. reuteri* ATCC 55730 has been shown to reduce the salivary levels of *Streptococcus* 

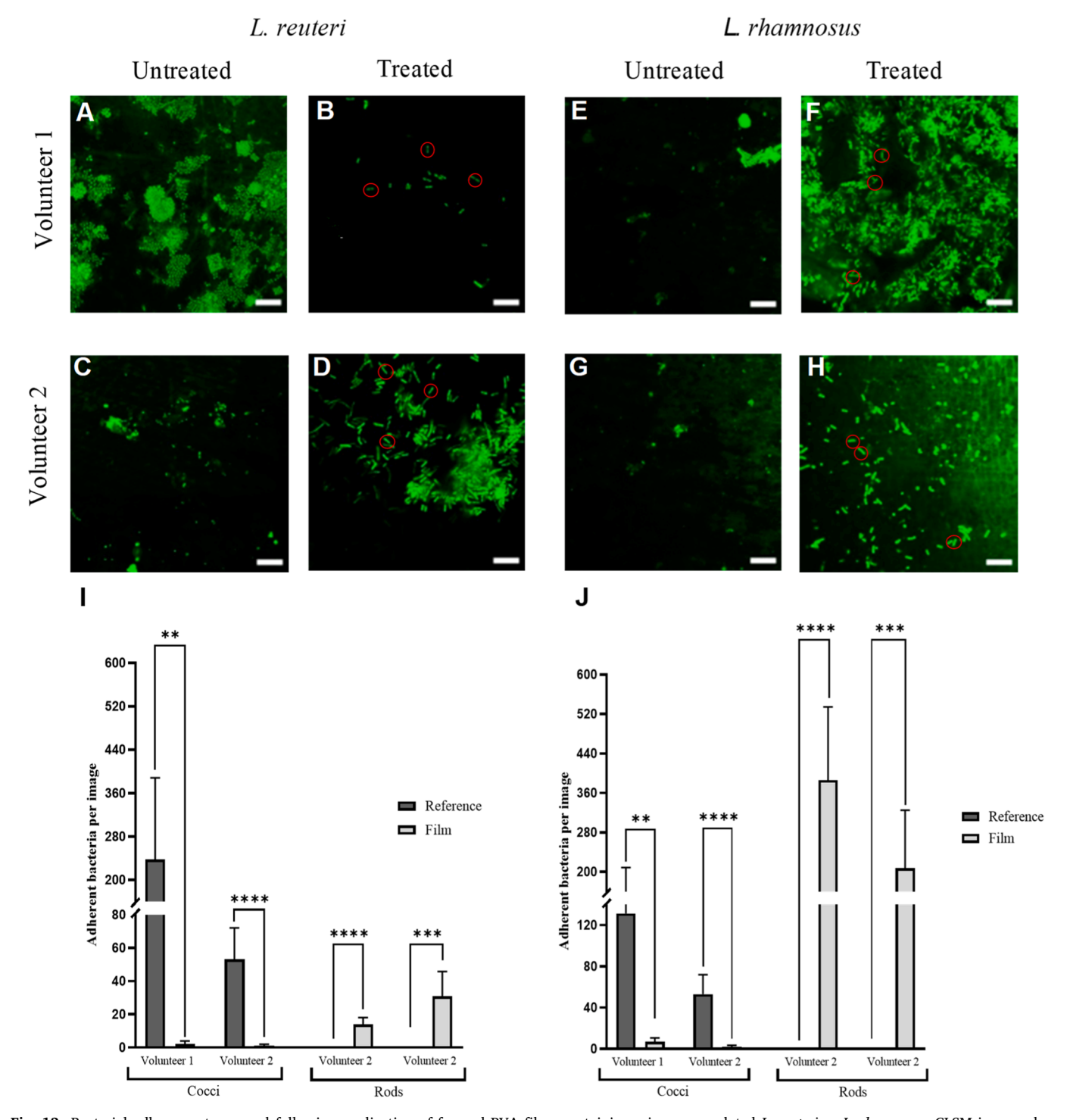


Fig. 13. Bacterial adherence to enamel following application of foamed PVA films containing microencapsulated L. reuteri or L. rhamnosus. CLSM images show enamel samples from two volunteers after 8 h of intraoral exposure. Panels A–D display samples for L. reuteri (A, B: untreated; C, D: treated), while panels E–H show samples for L. rhamnosus (E, F: untreated; G, H: treated). Panels I and J show the quantification of adherent coccoid and rod-shaped bacteria per image (8100  $\mu$ m²) for enamel specimens treated with films containing L. reuteri (panel I) and L. rhamnosus (panel J), respectively. Data are presented as mean  $\pm$  SD (n = 3). Statistical analysis was performed using unpaired two-tailed t tests. p < 0.01 (\*\*\*), p < 0.001 (\*\*\*), p < 0.001 (\*\*\*); p < 0.001

*mutans*, a key contributor to cariogenic biofilms [53]. These findings support the results of our study, where application of *L. reuteri*-loaded films led to a significant reduction in coccoid bacteria – morphologies typically associated with cariogenic species – and a simultaneous increase in rod-shaped lactobacilli on enamel surfaces.

#### 5. Conclusion

This study successfully developed and characterized mucoadhesive polymer films for the local delivery of L. reuteri and L. rhamnosus in the oral cavity. The films demonstrated strong mucoadhesion and robust mechanical properties, enabling practical handling and intraoral retention.

Spray drying enabled high initial bacterial survival, but the

incorporation of encapsulated bacteria into polymer films – particularly L. reuteri – resulted in substantial viability losses, highlighting a critical challenge in maintaining probiotic stability throughout processing. Microencapsulation did not preserve viability during film integration and, in some cases, reduced it.

Despite this, films containing microencapsulated probiotics showed significantly higher *in vivo* efficacy. They promoted enhanced adhesion of rod-shaped *lactobacilli* to enamel and effectively reduced coccoid bacteria associated with dysbiosis. The foamed PVA formulation was most effective, indicating that matrix architecture plays a key role in biological performance.

While the conventional HPMC-PVA films offered higher tensile strength and faster probiotic release, the foamed PVA structure allowed for greater bacterial loading and more sustained surface contact. These complementary characteristics suggest distinct application scenarios for each film type.

Overall, this work highlights that probiotic effectiveness cannot be evaluated by viability alone, but must be assessed under realistic biological conditions. The presented delivery system offers a promising approach for oral microbiome modulation and warrants further clinical investigation and formulation refinement.

#### CRediT authorship contribution statement

Marc Thiel: Investigation. Agnes-Valencia Weiss: Writing – review & editing, Supervision, Investigation. Christian Motz: Writing – review & editing. Karen Lienkamp: Writing – review & editing. Matthias Hannig: Writing – review & editing, Conceptualization. Marc Schneider: Writing – review & editing, Supervision, Resources, Conceptualization. Charlotte Eckermann: Writing – original draft, Investigation. Christof Johannes Klein: Writing – review & editing, Investigation, Formal analysis. Florian Schäfer: Writing – review & editing, Investigation.

### Declaration of Generative AI and AI-assisted technologies in the writing process

During the preparation of this work, the authors used ChatGPT 40 (OpenAI, May 2025 version) in order to improve the clarity, readability and language of the manuscript. After using this tool, the authors reviewed and edited the content as needed and take full responsibility for the content of the published article.

#### **Declaration of Competing Interest**

The authors declare the following financial interests/personal relationships which may be considered as potential competing interests: Marc Schneider reports a relationship with Lactopia GmbH that includes: consulting or advisory and equity or stocks. If there are other authors, they declare that they have no known competing financial interests or personal relationships that could have appeared to influence the work reported in this paper.

M.H. is co-founder of MooH GmbH, a company developing metagenomic based oral health tests.

#### Acknowledgements

This work was supported by Lactopia GmbH (Saarbrücken, Germany) and the Saarland University seed grant (Saarbrücken, Germany).

#### Data availability

Data will be made available on request.

#### References

- [1] L. Sedghi, V. DiMassa, A. Harrington, S.V. Lynch, Y.L. Kapila, The oral microbiome: Role of key organisms and complex networks in oral health and disease. Periodontology 2000, John Wiley and Sons Inc, 2021, pp. 107–131.
- [2] D. Verma, P.K. Garg, A.K. Dubey, Insights into the human oral microbiome. Archives of Microbiology, Springer Verlag, 2018, pp. 525–540.
- [3] M. Minty, T. Canceil, M. Serino, R. Burcelin, F. Tercé, V. Blasco-Baque, Oral microbiota-induced periodontitis: a new risk factor of metabolic diseases. Reviews in Endocrine and Metabolic Disorders, Springer, 2019, pp. 449–459.
- [4] N. Romani Vestman, P. Hasslöf, M.K. Keller, E. Granström, S. Roos, S. Twetman, C. Stecksén-Blicks, Lactobacillus reuteri influences regrowth of mutans streptococci after full-mouth disinfection: a double-blind, randomised controlled trial, Caries Res. 47 (2013) 338–345.
- [5] W. Teughels, A. Durukan, O. Ozcelik, M. Pauwels, M. Quirynen, M.C. Haytac, Clinical and microbiological effects of Lactobacillus reuteri probiotics in the treatment of chronic periodontitis: a randomized placebo-controlled study, J. Clin. Periodontol. 40 (2013) 1025–1035.
- [6] K. Lima-Engelmann, M. Schneider, Probiotic formulation development and local application with focus on local buccal, nasal and pulmonary application, Curr. Nutraceuticals 3 (2022).
- [7] M.L. Baca-Castañón, M.A. De la Garza-Ramos, A.G. Alcázar-Pizaña, Y. Grondin, A. Coronado-Mendoza, R.I. Sánchez-Najera, E. Cárdenas-Estrada, C.E. Medina-De la Garza, E. Escamilla-García, Antimicrobial effect of lactobacillus reuteri on cariogenic bacteria streptococcus gordonii, streptococcus mutans, and periodontal diseases actinomyces naeslundii and tannerella forsythia, Probiotics Antimicrob. Proteins 7 (2015) 1–8.
- [8] M.S. Kang, J.S. Oh, H.C. Lee, H.S. Lim, S.W. Lee, K.H. Yang, N.K. Choi, S.M. Kim, Inhibitory effect of Lactobacillus reuteri on periodontopathic and cariogenic bacteria, J. Microbiol. 49 (2011) 193–199.
- [9] D.F. Squarzanti, F. Dell'Atti, A.C. Scalia, Z. Najmi, A. Cochis, P. Malfa, Exploring the in vitro antibacterial potential of specific probiotic strains against oral pathogens, Microorganisms 12 (2024) 441.
- [10] L. Spaggiari, N. Pedretti, F. Ricchi, D. Pinetti, G. Campisciano, F.De Seta, M. Comar, S. Kenno, A. Ardizzoni, E. Pericolini, An untargeted metabolomic analysis of lacticaseibacillus (L.) rhamnosus, Lactobacillus (L.) acidophilus, lactiplantibacillus (L.) plantarum and Limosilactobacillus (L.) reuteri reveals an upregulated production of inosine from L. rhamnosus, Microorganisms 12 (2024) 662
- [11] F. Hodal E, P. Weinrich Karl, Probiotic oral dosage forms. Little Calumet Holdings, LLC. 2007.
- [12] Y.-H. How, S.-K. Yeo, Oral probiotic and its delivery carriers to improve oral health: a review, Microbiology (2021) 167.
- [13] S. Shanmugam, Oral films: a look back, Clin. Pharmacol. Biopharm. 05 (2016).
- [14] P.S. Avhad, R. Gupta, S.S. Rawat, R.S. Dubey, A glance on mucoadhesive system still more to understand, Res. J. Sci. Technol. 13 (2021) 133.
- [15] S.S. Rawat, A. Rai, D. Raina, I. Singh, Herbal bioactives-based mucoadhesive drug delivery systems, Adhes. Biomed. Appl. (2023) 121–149.
- [16] R. Jadhav, N. Kohale, G. Jawalkar, H. Sawarkar, Muco-adhesive buccal control delivery system, GSC Biol. Pharm. Sci. 29 (2024) 157–164.
- [17] I.M. Yermak, V.N. Davydova, A.V. Volod, 'ko, Mucoadhesive marine polysaccharides, Mar. Drugs 20 (2022) 522.
- [18] E.I. Rabea, M.E.T. Badawy, C.V. Stevens, G. Smagghe, W. Steurbaut, Chitosan as antimicrobial agent: applications and mode of action, Biomacromolecules 4 (2003) 1457–1465.
- [19] S. Verma, Polymers in designing the mucoadhesive films: a comprehensive review, Int. J. Green. Pharm. 12 (2018) 330.
- [20] A. Abruzzo, B. Vitali, F. Lombardi, L. Guerrini, B. Cinque, C. Parolin, F. Bigucci, T. Cerchiara, C. Arbizzani, M.C. Gallucci, B. Luppi, Mucoadhesive buccal films for local delivery of Lactobacillus brevis, Pharmaceutics 12 (2020).
- [21] N.P.R. Barro, L.M. Silva, G. Hassemer, E. Franceschi, R. Cansian, A. Junges, G. Toniazzo Backes, J. Zeni, R. Colet, M. Mignoni, E. Valduga, Microencapsulation of probiotic lactobacillus helveticus with different wall materials by spray drying, Biointerface Res. Appl. Chem. 11 (2021) 11221–11232.
- [22] F. Ansari, H. Pourjafar, V. Jodat, J. Sahebi, A. Ataei, Effect of Eudragit S100 nanoparticles and alginate chitosan encapsulation on the viability of Lactobacillus acidophilus and Lactobacillus rhamnosus, AMB Express 7 (2017) 144.
- [23] Y. Miyoshi, S. Okada, T. Uchimura, E. Satoh, A mucus adhesion promoting protein, mapa, mediates the adhesion of lactobacillus reuteri to caco-2 human intestinal epithelial cells, Biosci. Biotechnol. Biochem. 70 (2006) 1622–1628.
- [24] F. Rahmati, Microencapsulation of Lactobacillus acidophilus and Lactobacillus plantarum in Eudragit S100 and alginate chitosan under gastrointestinal and normal conditions, Appl. Nanosci. 10 (2020) 391–399.
- [25] H. Oliveira, M. Costa, J. Soares, Investigation of lactobacillus paracasei encapsulation in electrospun fibers of Eudragit® L100, Polímeros 30 (2020). E2020025.
- [26] M. Yao, J. Xie, H. Du, D.J. McClements, H. Xiao, L. Li, Progress in microencapsulation of probiotics: a review, Compr. Rev. Food Sci. Food Saf. 19 (2020) 857–874.
- [27] C. Eckermann, C.J. Klein, C. Lasch, A. Luzhetskyy, M. Schneider Development of Mucoadhesive Polymer Films as a Delivery System for Microencapsulated Lactobacillus reuteri – Strategies to Improve Bacterial Viability, Next Research, (in reply).
- [28] Y. Takeuchi, N. Ikeda, K. Tahara, H. Takeuchi, Mechanical characteristics of orally disintegrating films: comparison of folding endurance and tensile properties, Int. J. Pharm. 589 (2020) 119876.

- [29] B. Yir-Erong, B.M. T, A. Isaac, G.S. Y, J.S, Boateng, Oral thin films as a remedy for noncompliance in pediatric and geriatric patients, Ther. Deliv. 10 (2019) 443–464.
- [30] 2018, ISO 527-3:2018.
- [31] G.B. Proctor, The physiology of salivary secretion. Periodontology 2000, Blackwell Munksgaard, 2016, pp. 11–25.
- [32] M. Hannig, Transmission electron microscopy of early plaque formation on dental materials in vivo, Eur. J. ORAL Sci. 107 (1999).
- [33] D.M. Rajaram, S.D. Laxman, Buccal mucoadhesive films: a review, Syst. Rev. Pharm. (2016) 31–38.
- [34] V.B. Lordello, A.B. Meneguin, S.R. de Annunzio, M.P. Taranto, M. Chorilli, C. R. Fontana, D.C.U. Cavallini, Orodispersible film loaded with enterococcus faecium CRL183 presents anti-candida albicans biofilm activity in vitro, Pharmaceutics 13 (2021) 998.
- [35] J. Schmitz, E. Manevich, M. Tschöpe, R. Alon, K.E. Gottschalk, Linking single integrin–ligand bond properties to cell adhesiveness under external forces exemplified by the VLA-4–VCAM-1 bond, Soft Matter (2009).
- [36] S. Alaei, H. Omidian, Mucoadhesion and mechanical assessment of oral films, Eur. J. Pharm. Sci. 159 (2021) 105727.
- [37] S. Alaei, H. Omidian, Mucoadhesion and Mechanical Assessment of Oral Films. European Journal of Pharmaceutical Sciences, Elsevier B.V, 2021.
- [38] M. Davidovich-Pinhas, H. Bianco-Peled, Mucoadhesion: a review of characterization techniques, Expert Opin. Drug Deliv. (2010) 259–271.
- [39] V.V. Khutoryanskiy, Advances in mucoadhesion and mucoadhesive polymers, Macromol. Biosci. 11 (2011) 748–764.
- [40] Q.D. Pham, S. Nöjd, M. Edman, K. Lindell, D. Topgaard, M. Wahlgren, Mucoadhesion: mucin-polymer molecular interactions, Int. J. Pharm. (2021) 610.
- [41] J. Bohn, A. Yüksel-Dadak, S. Dröge, H. König, Isolation of lactic acid-forming bacteria from biogas plants, J. Biotechnol. 244 (2017) 4–15.
- [42] A. Abdkader, P. Penzel, D. Friese, M. Overberg, L. Hahn, M. Butler, V. Mechtcherine, C. Cherif, Improved tensile and bond properties through novel rod constructions based on the braiding technique for non-metallic concrete reinforcements, Materials 16 (2023).

- [43] B.D. Sahm, A.B.V. Teixeira, A.C. dos Reis, Graphene loaded into dental polymers as reinforcement of mechanical properties: A systematic review. Japanese Dental Science Review, Elsevier Ltd, 2023, pp. 160–166.
- [44] N. Wiemer, A. Wetzel, M. Schleiting, P. Krooß, M. Vollmer, T. Niendorf, S. Böhm, B. Middendorf, Effect of fibre material and fibre roughness on the pullout behaviour of metallic micro fibres embedded in UHPC, Materials 13 (2020).
- [45] (Dd) J. Espinosa-Martínez, X. Aparicio-Fernández, C. Ramírez-López, P. Hernández-Carranza, I.I. Ruiz-López, C.E. Ochoa-Velasco, Application of functional edible films with antioxidant, probiotic, and antimicrobial properties on Mexican sweet potato candy, Int. J. Food Sci. Technol. 60 (2025).
- [46] R.J.B. Heinemann, R.A. Carvalho, C.S. Favaro-Trindade, Orally disintegrating film (ODF) for delivery of probiotics in the oral cavity - Development of a novel product for oral health, Innov. Food Sci. Emerg. Technol. 19 (2013) 227–232.
- [47] M.B. Rebelo, C.S. Oliveira, F.K. Tavaria, Development of a postbiotic-based orodispersible film to prevent dysbiosis in the oral cavity, Front. Biosci. 17 (2025).
- [48] P. Kanmani, S.T. Lim, Development and characterization of novel probioticresiding pullulan/starch edible films, Food Chem. 141 (2013) 1041–1049.
- [49] S.Abu Baker, M. El-Barrawy, E. Omran, H. Raslan, Occurrence of some oral potentially pathogenic microorganisms and their associated risk factors, J. High. Inst. Public Health 47 (2017) 69–75.
- [50] J.-Y. Ren, H.-Q. Yu, S. Xu, W.-J. Zhou, Z.-H. Liu, Putative pathogenic factors underlying Streptococcus oralis opportunistic infections, J. Microbiol. Immunol. Infect. 58 (2025) 157–163.
- [51] S. Bloch, F.F. Hager-Mair, O. Andrukhov, C. Schäffer, Oral streptococci: modulators of health and disease, Front. Cell. Infect. Microbiol. 14 (2024) (2024).
- [52] L. Rimondini, M. Fini, R. Giardino, The microbial infection of biomaterials: a challenge for clinicians and researchers. a short review, J. appl. Biomater. Biomech. JABB 3 (2005) 1–10.
- [53] Z. Liu, Q. Cao, W. Wang, B. Wang, Y. Yang, C.J. Xian, T. Li, Y. Zhai, The Impact of Lactobacillus reuteri on Oral and Systemic Health, A Compr. Rev. Recent Res. 13 (2025) 45.